Universal scaling properties of type-I intermittent chaos in isolated resistance arteries are unaffected by endogenous nitric oxide synthesis

D. Parthimos, D. H. Edwards, and T. M. Griffith*
Department of Diagnostic Radiology, Wales Heart Research Institute, University of Wales College of Medicine, Heath Park, Cardiff CF14 4XN, United Kingdom
(Received 4 May 2001; published 20 November 2001)

Spontaneous fluctuations in flow in isolated rabbit ear resistance arteries may exhibit almost-periodic behavior interrupted by chaotic bursts that can be classified as type-I Pomeau-Manneville intermittency. This conclusion was supported by the construction of parabolic return maps and identification of the characteristic probability distributions for the number of oscillations per laminar segment (n) associated with the type-I scenario. Pharmacological inhibition of nitric oxide (NO) synthesis by the vascular endothelium modulated the dynamics of the reinjection mechanism, and thus the generic shape of the probability distribution for n. Nevertheless, average laminar length was related to a derived bifurcation parameter ε according to power-law scaling of the form $\langle n\rangle \sim \varepsilon^{\beta}$, where the estimated critical exponent β was close to the theoretical value of -0.5 both in the presence and absence of NO synthesis.

DOI: 10.1103/PhysRevE.64.061906 PACS number(s): 87.19.−j, 05.45.−a

Intermittency has been extensively studied as one of the established routes to chaos, and a variety of universal classes, including types I, II, III [1–3], ''crisis-induced'' [4] and ''on-off'' [5], have been characterized theoretically and observed experimentally in physical systems. We have previously demonstrated type-III intermittency, in which intermittent laminar dynamics arises at a subcritical period-doubling bifurcation, in the spontaneous oscillations in flow observed in isolated arteries following administration of histamine [6]. Such intrinsic rhythmic contractile activity is known as vasomotion, and is thought to contribute to the optimization of microcirculatory perfusion [7–11].

In the present study we provide evidence that vasomotion can also exhibit patterns of type-I intermittent chaos by measuring flow in first generation ear arteries, ~1 cm in length and ~150 μm in diameter, isolated from male New Zealand White rabbits [6,12]. These vessels were perfused at a mean flow of 0.5 ml/min with fluctuations about the mean caused by intrinsic rhythmic contractile activity being monitored by a transonic probe (Transonic Systems, type 2N, sampling frequency 4 Hz) included in series with the perfusion circuit as previously described [6,12]. Experimental and modelling studies have shown how vasomotion is generated at the level of the smooth muscle cell and involves nonlinear interactions between cytosolic and membraneous oscillators that together regulate intracellular Ca^{2+} [12–14]. The patterns of vasomotion observed experimentally in rabbit ear arteries can be modulated by N^G-nitro-L-arginine methyl ester (L-NAME), which blocks the synthesis of NO by the endothelial monolayer that lines the vessel wall. This endogenous relaxing factor regulates the contractile behavior of vascular smooth muscle, but does not affect the intrinsic complexity of vasomotion as assessed by calculation of the Grassberger-Proccacia correlation dimension [12,13].

According to Pomeau and Manneville, type-I intermittency is associated with a reverse tangent (saddle node) bifurcation, in which the eigenvalues of the Floquet matrix of a fixed point pass through the unit circle. This generates a laminar phase characterized by a sequence of almost periodic oscillations that begins when a chaotic trajectory is injected into the vicinity of the saddle bifurcation bottleneck and ends when the dynamics is ejected from the map. These sequences of almost periodic oscillations either increase or decrease in amplitude in a slow monotonic fashion, a property that can be used to identify the initiation and termination of the laminar regime. The successive maxima x_n present in this regime conform to a universal mapping $x_n \rightarrow x_{n+1}$ described by

$$x_{n+1} = \varepsilon + x_n + \alpha x_n^2, \tag{1}$$

where ε is a small bifurcation parameter determining the width of the laminar channel of the return map. As ε increases, so does the width of the channel, resulting in ever shorter laminar lengths (i.e., number of successive almost periodic oscillations) interspersed with more frequent chaotic bursts. Traces from two different arteries exhibiting intermittent fluctuations in flow are shown in Fig. 1 along with first return maps of successive maxima derived from the laminar sections of each experimental trace. The return maps thus derived conform to the parabolic return map characteristic of type-I intermittency described by Eq. (1), with least squares error fits yielding $\varepsilon = 0.011 \pm 0.001$ and 0.013 ± 0.001. Inspection of Fig. 1 shows that the amplitude of successive oscillations increases in trace (a) but decreases in trace (b). This is reflected in the corresponding return maps, where the parabolic fits appear on opposite sides of the line of identity. Trace (a) was obtained after the administration of 2.5 μM histamine, whereas trace (b) was produced after the administration of both 2.5 μM histamine and 50 μM L-NAME, thus suggesting that differences in the dynamics of the two oscillatory patterns and their associated return maps are directly attributable to altered NO activity.

*Author to whom correspondence should be addressed. Email address: griffith@cardiff.ac.uk

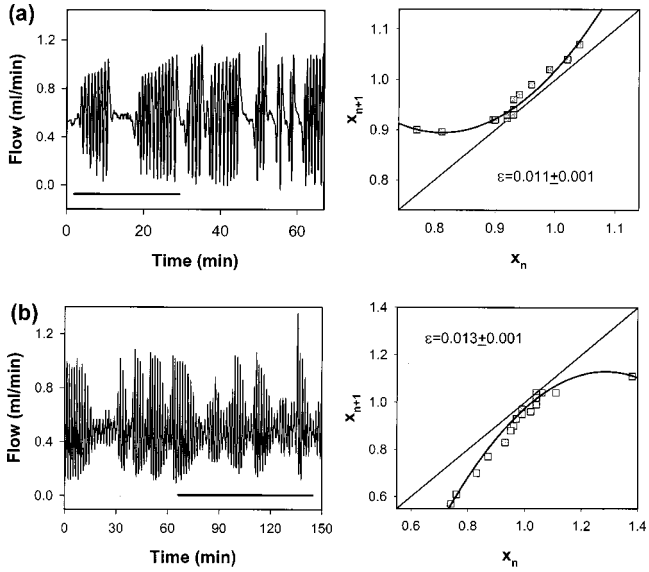

FIG. 1. (a, b) Two representative examples of vasomotion in isolated rabbit ear arteries exhibiting intermittency. The vessels were perfused at a time-averaged flow rate of 0.5 ml/min in the presence of 2.5 μM histamine to activate vascular smooth muscle with fluctuations in flow monitored continuously by a transonic probe. Vessel (b) was also perfused with 50 μM N^G-nitro-L-arginine methyl ester (L-NAME) to inhibit nitric oxide synthesis by the vascular endothelium. Return maps were constructed by plotting successive maxima (x_n vs x_{n+1}) from the laminar oscillatory segments of the signals as indicated on each trace by an underlying bar. In both cases parabolic fits are consistent with the type-I Pomeau-Manneville scenario: (a) above the line of identity, and (b) below the line of identity. Bifurcation parameters ε were calculated by least squares error fits.

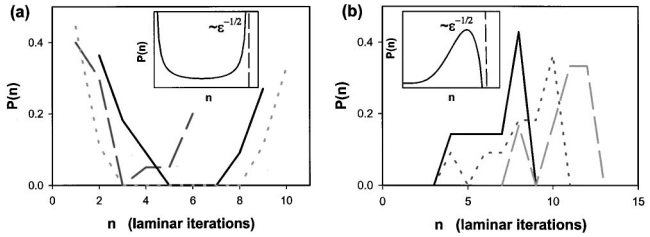

FIG. 2. Normalized probability distributions for laminar segment containing n oscillations in arteries exhibiting intermittency for a minimum of 70 min. For clarity, only six examples are presented because of overlap, and were grouped into two families that have both been theoretically associated with type-I Pomeau-Manneville intermittency (insets). (a) U-shape distributions. (b) Distribution curve generally increasing with laminar length but delimited by an abrupt cutoff. The existence of more than a single peak [e.g., dashed lines in (b)] may be attributable to the presence of biological noise [17]. Distributions of the form shown in panels a and b were obtained in the presence and absence of NO synthesis, respectively.

The number of iterations n undertaken by a representative trajectory before it exits from the laminar channel of the parabolic map depends on the distance from the unstable monoperiodic point at which reinjection occurs after the previous chaotic burst. This iteration length can be estimated by approximating Eq. (1) in the continuous form [1–3]

$$\frac{dx}{dn} = \varepsilon + \alpha x^2. \tag{2}$$

Integration gives

$$x(\varepsilon, n_0) \sim (\varepsilon/\alpha)^{1/2} \tan\{(\varepsilon\alpha)^{1/2}[n - n_0]\}, \tag{3}$$

where n_0 is the iteration step at which the trajectory passes nearest the most narrow part of the laminar channel. The number of iterations in the laminar region (i.e., the laminar length) is, therefore, given by

$$n = \frac{1}{\sqrt{\alpha\varepsilon}} \left(\arctan\left[\frac{x_{\text{out}}}{\sqrt{\varepsilon/\alpha}} \right] - \arctan\left[\frac{x_{\text{in}}}{\sqrt{\varepsilon/\alpha}} \right] \right), \tag{4}$$

where the subscripts denote the location of the entry and exit points of the dynamics in the laminar channel. It is evident from Eq. (3) that $x(\varepsilon, n_0)$ diverges for $n - n_0 = (\pi/2)\varepsilon^{-1/2}$. Thus, for a given ε the maximum number of oscillations found in a laminar sequence would be expected to exhibit an abrupt cutoff at an upper bound $\sim \varepsilon^{-1/2}$ [1–3]. In practice, this upper bound can be estimated by constructing the normalized probability distribution $P(n)$ for laminar lengths containing n oscillations. The exact shape of this distribution is, however, influenced by the dynamics of the reinjection mechanism. Indeed, in the literature two theoretical curves have been associated with type-I intermittency: (i) a U-shape distribution that is generated by a uniform reinjection into the channel with trajectories rejoining the laminar section both before and after the bottleneck [15–17], and (ii) a monotonically increasing probability distribution in which reinjection occurs largely before the bottleneck so that most trajectories traverse the full length of the channel [1,2]. Probability distributions for the length of the laminar segments derived from arteries exhibiting sustained intermittent behavior for >70 min supported both of these theoretical predictions (Fig. 2). Thus, from a total of 13 arteries the probability distribution was U shaped in five cases with observations being concentrated at short and long laminar lengths, a pattern found only in arteries perfused with histamine under control conditions. By contrast, in the remaining eight vessels, in which NO synthesis was blocked by L-NAME, the probability distribution generally increased before an abrupt cutoff at long laminar lengths.

To illustrate the close association of these two distinct intermittency regimes, Fig. 3 shows the effects of blockade of NO synthesis by L-NAME in a single artery. Segments (a) and (b) exhibit two dynamically distinct patterns similar to those observed in Fig. 1(a) and Fig. 1(b) in different arteries. Changes in the underlying dynamics were analyzed by constructing first maximum return maps that revealed two distinct clusters of points on the plane [Fig. 3(c)]. It is evident that due to the action of L-NAME the return map has shifted from one type-I intermittent regime to another in the vicinity of a new saddle-bifurcation origin. In order to visualize differences between the two intermittent regimes in a higher dimensional space, their underlying dynamical attractors

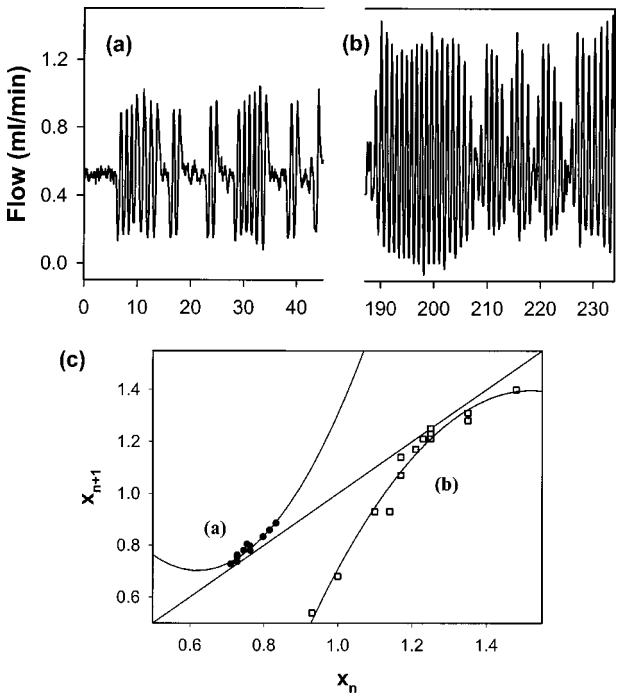

FIG. 3. Fluctuations in flow recorded in the same artery under control conditions and after administration of L-NAME to inhibit endothelial NO synthesis. (a) In the presence of 2.5 μM histamine, and (b) in the presence of both 2.5 μM histamine and 50 μM L-NAME. (c) Return map for successive maxima within the laminar segments (a) and (b) of the experimental time series. Least squares parabolic fits gave $\varepsilon = 0.022 \pm 0.01$ and 0.018 ± 0.005, respectively.

were reconstructed by time-delayed embedding, according to the method of Rosenstein and co-workers [18] in which a measure of attractor ''space-filling'' (i.e., average displacement between points) is computed as a function of time delay τ according to

$$S(\tau) = \frac{1}{M} \sum_{i=1}^{M} \sqrt{\sum_{j=0}^{m-1} (x_{i+j\tau} - x_i)^2}, \tag{5}$$

where M is the number of points x_i in the data set and m denotes the dimension of the embedding. For small values of τ the points of the attractor remain closely packed. On increasing τ the average displacement of the points of the attractor increases to a plateau when the attractor is fully unfolded. The optimum time delay for unfolding the attractor is determined at the point where the slope of the $S(\tau)$ plot (as a function of τ) decreases by 40% from the initial value obtained with $\tau = 1$. For the traces in Fig. 3(a) and Fig. 3(b), optimal values of τ obtained by this method were ~6 and ~7 sec, respectively, and used to reconstruct the attractors shown in Fig. 4. It is evident that the band of the attractor corresponding to the intermittent laminar regime of Fig. 4(a) is much narrower than the equivalent band in the attractor shown in Fig. 4(b), although the width of the band corresponding to reinjection is similar in both instances. In the former case, the width of the reinjection band is almost equal to the width of the laminar regime and will thus result in a relatively uniform reinjection, whereas the width of the rein-

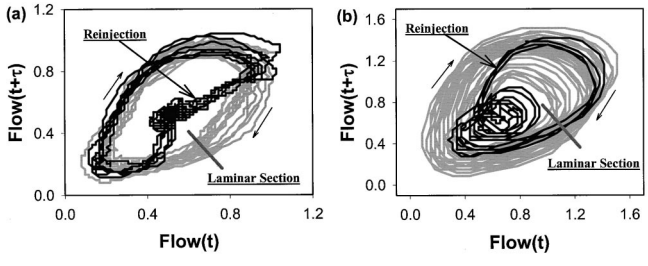

FIG. 4. (a), (b) Two-dimensional dynamical attractors constructed by time-delayed embedding of the traces shown in panels (a) and (b) of Fig. 3, respectively. The laminar and reinjection regimes and the direction of the trajectories are indicated.

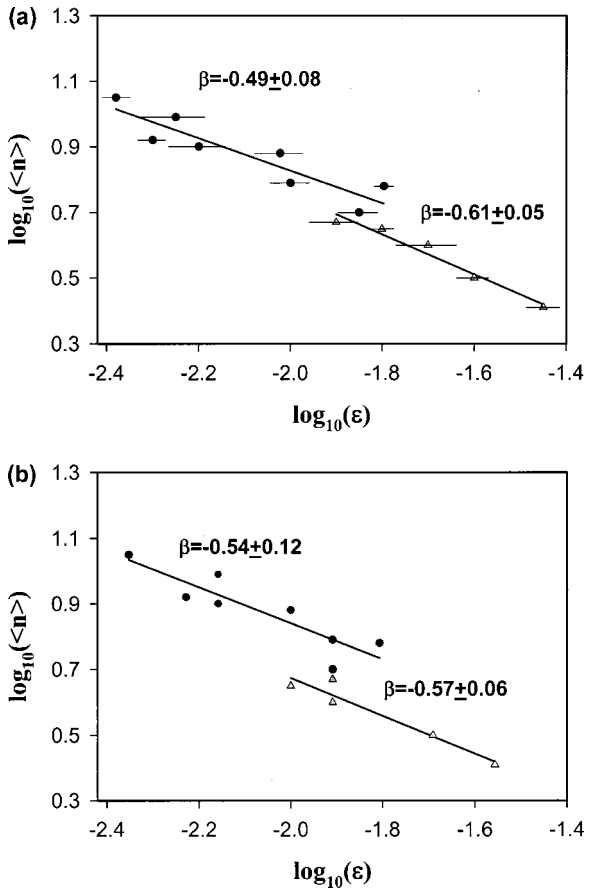

FIG. 5. Relationship between the average number of oscillations per laminar segment and the bifurcation parameter ε for 13 individual arteries. In (a) ε is calculated from the return map parabolic fits, whereas in (b) ε is calculated from the cutoff point of the laminar length probability distribution. In both cases two distinct groups of points have been distinguished: those corresponding to the U-shaped probability distribution of Fig. 2(a), which are derived from arteries perfused with 2.5 μM histamine alone (open triangles), and those corresponding to the probability distributions of Fig. 2(b), which were derived from arteries perfused with both 2.5 μM histamine and 50 μM L-NAME (closed circles). The linearity of the plots is consistent with critical scaling according to $\langle n \rangle \sim \varepsilon^{\beta}$ where β is a universal power exponent. Least squares fits gave values of the exponent β close to the theoretical value of -0.5 cited in the literature for type-I intermittency.

jection band in the latter case is much narrower than the band corresponding to the laminar regime, thus leading to nonuniform reinjection. This example illustrates how the two classes of probability distribution discussed above may be observed in the same experimental system.

Further confirmation of the type-I intermittent scenario was obtained by relating the average number of oscillations in each laminar segment $\langle n \rangle$ to the bifurcation parameter ε. Two complementary methods were employed to derive these plots from the experimental data: (i) calculation of ε from parabolic return maps and (ii) relating the cutoff in the probability distributions to $\varepsilon^{-1/2}$ as discussed above. Figure 5 demonstrates that a consistent scaling relationship exists when estimates of ε, derived from either method, are plotted against $\langle n \rangle$ for individual arteries on a double logarithmic scale, even though ε was generally smaller and $\langle n \rangle$ larger in the presence of NO synthesis. In panel (a), where ε was calculated by method (i), data from the five arteries in which the laminar length probability distribution was U shaped are plotted as open triangles and exhibit a good power law fit of the form $\langle n \rangle \sim \varepsilon^{\beta}$ with β estimated by linear regression as -0.61 ± 0.05. Corresponding data from the eight arteries in which the probability distribution was similar to that of Fig. 2(b) are plotted as closed circles with β estimated as -0.49 ± 0.08. In panel (b), following method (ii), the same data reproduced the power law fit with β estimated by linear regression as -0.57 ± 0.06 for the U-shaped probability distributions and -0.54 ± 0.12 for the distributions exhibiting an abrupt cutoff. The findings consequently reveal the existence of a universal critical scaling phenomenon with a scaling exponent that is insensitive to the presence or absence of NO synthesis and thus to the exact mechanism of reinjection.

Similar values of β have been reported for type-I intermittency in precisely controllable physical systems such as a four-level coherently pumped molecular laser with $\beta = -0.52$ [19], a single-mode ring laser with $\beta = -0.60 \pm 0.03$ [20] and a driven nonlinear semiconductor oscillator with two scaling regimes with slopes of -0.45 ± 0.05 and -0.65 ± 0.05 [21]. Theoretical studies with coupled logistic maps [22] and the renormalization group approach [23] have shown that if a significant proportion of the trajectories in the reinjection band join the laminar segment before the narrowest point critical scaling occurs in two distinct linear segments with slopes 0 and -0.5. However, if most reinjection trajectories meet the laminar channel at or after its narrowest point, there may be a single scaling region with a theoretical slope of -0.5.

The bifurcation parameter ε in type-I intermittency may be considered as a displacement from a critical point of the form $\varepsilon = (\mu - \mu_c)/\mu_c$, where μ is a control parameter and μ_c is its value at the fixed point where the saddle bifurcation originates. In physical systems, the control parameter μ can be directly related to a variable such as resonator detuning and pump field strength in lasers, magnetic field strength in plasma physics or semiconductors or resistance in electrical circuits [19,20,24–26]. In such systems, μ can be adjusted to reveal an often complex return map, with slight variations in μ resulting in translation of the map without significant loss of its salient dynamical features [15,19,21,24,26]. In vasomotion, however, the nature of the bifurcation parameter ε is unknown so that it cannot be manipulated in a controlled fashion. Nevertheless, the present results demonstrate that pharmacological perturbation of NO synthesis may cause a translation of the return map such that the initial intermittent channel disappeared and another intermittent channel became active in a different regime of the map [Fig. 3(c)].

In conclusion, observations of type-I intermittency extend previous studies showing that the ''macroscopic'' behavior of the arterial wall, which may be regarded as a spatially-extended system consisting of a large number of coupled cells, can exhibit patterns of nonlinear oscillatory activity that can be described by discrete one-dimensional return maps [6,27]. Pharmacological manipulation of NO synthesis modified the dynamics of reinjection but did not fundamentally affect the critical scaling relationship that characterizes type-I intermittency.

This work was supported by the Medical Research Council.

[1] P. Manneville and Y. Pomeau, Physica D **1**, 219 (1980).
[2] Y. Pomeau and P. Manneville, Commun. Math. Phys. **74**, 189 (1980).
[3] H. Schuster, *Deterministic Chaos* (VCH, Weinheim, Germany, 1989).
[4] C. Grebogi, E. Ott, F. J. Romeiras, and J. A. Yorke, Phys. Rev. A **36**, 5365 (1987).
[5] N. Platt, E. A. Spiegel, and C. Tresser, Phys. Rev. Lett. **70**, 279 (1993).
[6] T. M. Griffith, D. Parthimos, J. Crombie, and D. H. Edwards, Phys. Rev. E **56**, R6287 (1997).
[7] T. W. Secomb, M. Intaglietta, and J. F. Gross, Prog. Appl. Microcirc. **15**, 49 (1989).
[8] T. C. Skalak, G. W. Schmid-Schönbein, and B. W. Zweifach, Microvasc. Res. **28**, 95 (1984).
[9] E. R. Clark and E. L. Clark, Am. J. Anat. **49**, 441 (1932).
[10] T. M. Griffith, Cardiovasc. Res. **31**, 342 (1996).
[11] D. Parthimos, D. H. Edwards, and T. M. Griffith, Cardiovasc. Res. **31**, 388 (1996).
[12] T. M. Griffith and D. H. Edwards, Am. J. Physiol. **266**, H1786 (1994).
[13] T. M. Griffith and D. H. Edwards, Am. J. Physiol. **266**, H1801 (1994).
[14] D. Parthimos, D. H. Edwards, and T. M. Griffith, Am. J. Physiol. **277**, H1119 (1999).
[15] R. Richter, A. Kittel, G. Heinz, G. Flatgen, J. Peinke, and J. Parisi, Phys. Rev. B **49**, 8738 (1994).
[16] H. Kaplan, Phys. Rev. Lett. **68**, 553 (1992).
[17] J. E. Hirsch, B. A. Huberman, and D. J. Scalapino, Phys. Rev. A **25**, 519 (1982).
[18] M. T. Rosenstein, J. J. Collins, and C. J. De Luca, Physica D **73**, 82 (1994).

[19] M. Arjona, J. Pujol, and R. Corbalan, Phys. Rev. A **50**, 871 (1994).
[20] D. Y. Tang, M. Y. Li, and C. O. Weiss, Phys. Rev. A **46**, 676 (1992).
[21] C. Jeffries and J. Perez, Phys. Rev. A **26**, 2117 (1982).
[22] C-M. Kim, O. J. Kwon, E-K. Lee, and H. Lee, Phys. Rev. Lett. **73**, 525 (1994).
[23] O. J. Kwon, C-M. Kim, E-K. Lee, and H. Lee, Phys. Rev. E **53**, 1253 (1996).
[24] D. L. Feng, J. Zheng, W. Huang, and C. X. Yu, Phys. Rev. E **54**, 2839 (1996).
[25] J. Perez and C. Jeffries, Phys. Lett. **92A**, 82 (1982).
[26] C-M. Kim, G-S. Yim, Y. S. Kim, J-M. Kim, and H. W. Lee, Phys. Rev. E **56**, 2573 (1997).
[27] S. De Brouwer, D. H. Edwards, and T. M. Griffith, Am. J. Physiol. **274**, H1315 (1998).